

LARGE ELASTIC COMPRESSION OF FINITE RECTANGULAR BLOCKS OF RUBBER

By JAMES M. HILL and ALEXANDER I. LEE

(Department of Mathematics, University of Wollongong, Wollongong,
New South Wales, Australia)

[Received 16 March 1988]

SUMMARY

For the problem of large elastic compression of a finite rectangular rubber block which has bonded metal plates to its upper and lower surfaces, a new load-deflection relation is derived assuming an isotropic incompressible Mooney material and that the pointwise vanishing of the stress on the free faces can be replaced by the vanishing of the force resultant on these faces. The load-deflection relation so obtained is derived from a fully three-dimensional deformation which is a generalization of a plane-strain deformation given previously for infinitely long rectangular rubber pads. The 'finite' and 'infinite' load-deflection relations are compared with experimental results and with that predicted by the conventional engineering approximation deduced from the so-called 'shape-factor' method.

1. Introduction

THE problems arising from large elastic deformations of finite rectangular rubber blocks are still important and relevant both to the construction engineer, who utilizes such devices in bridges for example, and to the manufacturer of rubber engineering components, both of whom need to predict accurately their *in situ* mechanical performance. Typically such devices have bonded metal plates on their upper and lower surfaces and the three principal deformation modes of most concern are compression, shearing and tilting (rotational) which are effected by fixing the lower metal plate and applying forces or moments to the upper plate as indicated in Fig. 1. In this paper we consider the problem of large elastic compression of bonded finite rectangular blocks of rubber which is assumed to be the isotropic incompressible perfectly elastic Mooney material.

Since the problem involves finite deformations there is no exact solution and much of the engineering literature is based on load-deflection relations of the type emanating from the linear theory of elasticity but couched in terms of the 'shape factor' S which is defined by

$$S = \frac{\text{one loaded area}}{\text{force-free area}}, \quad (1.1)$$

and incorporating an 'apparent Young's modulus' E_a which varies with S .

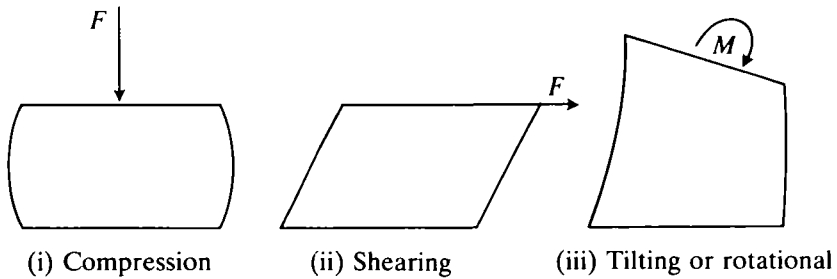


FIG. 1

For compression the resulting force-deflection relation arising from integrating the equation

$$\frac{dF}{d\delta} = \frac{(\text{apparent Young's modulus}) \times (\text{one loaded area})}{(\text{thickness after a compression of magnitude } \delta)}, \quad (1.2)$$

where F is the applied force, frequently provides a surprisingly accurate description of the actual behaviour of bonded rubber blocks. Such analysis has no rational or continuum mechanical basis and its apparent success derives from the fact that the assumed relations are fudged to fit experimental results. For many engineering purposes such a superficial analysis may be perfectly adequate. However, it only conveys reasonably accurate information about the force-deflection relation which is a macroscopic property of the block. It provides no information whatsoever on the pointwise variation of stresses and deformation throughout the block. Further, the extension to slightly more sophisticated problems is by no means obvious and depends upon whether there already exists a substantial body of experimental results on the problem. Thus although the shape-factor approach by no means describes the whole story, it must nevertheless be compared and considered in the context of any new proposed force-deflection relation. For the shape-factor approach and the engineering literature relating to this method we refer the reader to Gent and Lindley (1).

In order to provide a rational framework for the derivation of load-deflection relations, Klingbeil and Shield (2) produced an approximate solution for infinitely long rectangular blocks assuming firstly that material planes $Y = \text{constant}$ are mapped into planes $y = \text{constant}$ (see Fig. 2) and secondly that the pointwise requirement of zero stress on the free surfaces is replaced by the vanishing of resultant forces on these surfaces. Accordingly for the isotropic incompressible perfectly elastic Mooney material, Klingbeil and Shield (2) exploited solutions of the form

$$x = f(Y)X, \quad y = g(Y), \quad z = Z, \quad (1.3)$$

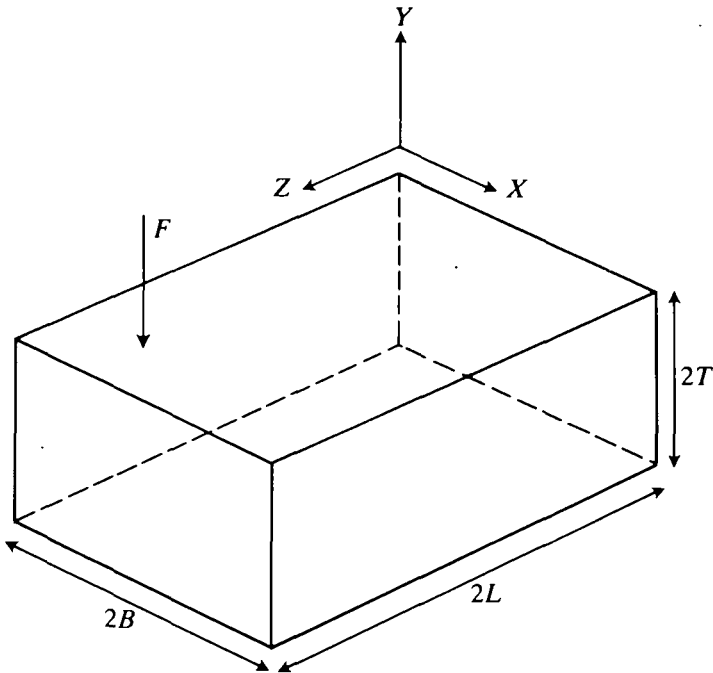


FIG. 2

where (X, Y, Z) and (x, y, z) denote material and spatial rectangular Cartesian coordinates respectively. Further, $f(Y)$ and $g(Y)$ denote functions of Y only which are determined completely from the constraint of incompressibility, the equilibrium equations and appropriate displacement boundary conditions. The resulting load-deflection relation provides a reasonably accurate representation of experimental behaviour. In practice however, rectangular rubber blocks tend not to be particularly long in one direction and the purpose of this paper is to investigate a possible three-dimensional extension of the solution of Klingbeil and Shield (2).

Accordingly for the Mooney material we adopt a deformation of the form

$$x = f(Y)X, \quad y = g(Y), \quad z = h(Y)Z, \quad (1.4)$$

and now, based on the assumption that the vanishing of pointwise stresses on four free faces can be replaced by the vanishing of two resultant forces, we may deduce yet another force-deflection relation. In this paper we examine the three force-deflection relations arising from the shape-factor method, (2) and the deformation (1.4) and we make a comparison with experimental results. In the next three sections of the paper we give respectively the basic equations for finite deformations of a Mooney

material, the solutions for the deformation (1.4) and the approximate analysis leading to the load-deflection relation for compression of rectangular rubber blocks of finite length. In section 5 we give the corresponding linear estimate which we relate to that arising from the shape-factor method and in section 6 we compare the various load-deflection relations with experimental results.

2. Basic equations for finite elastic deformations of a Mooney material

For fully three-dimensional deformations of the isotropic incompressible perfectly elastic Mooney material the calculations associated with the equilibrium equations are frequently awkward and involved. One approach which minimizes the labour is to exploit the 'reciprocal equations' given by Hill (3, 4). Such equations utilize both the deformation and its inverse. Thus with material and spatial rectangular cartesian coordinates Z^K ($K = 1, 2, 3$) and z^j ($j = 1, 2, 3$) respectively, the deformation and its inverse take the form

$$z^j = z^j(Z^K), \quad Z^K = Z^K(z^j), \quad (2.1)$$

with strain tensors

$$c^{-1ij} = \frac{\partial z^i}{\partial Z^K} \frac{\partial z^j}{\partial Z^K}, \quad c^{ij} = \frac{\partial Z^K}{\partial z^i} \frac{\partial Z^K}{\partial z^j}, \quad (2.2)$$

where as usual the repeated index implies summation. The Mooney strain-energy function is given by

$$\Sigma = C_1(I_1 - 3) + C_2(I_2 - 3), \quad (2.3)$$

where C_1 and C_2 are material constants and I_1 and I_2 are the traces of the matrices c^{-1} and c respectively. From either of (3, 4) we may readily deduce the reciprocal equations for the deformation (2.1) of a Mooney material,

$$\frac{\partial}{\partial z^i} (p + C_2 I_2) = 2C_1 \nabla^2 z^i - 2C_2 \frac{\partial Z^K}{\partial z^i} \nabla_1^2 Z^K, \quad (2.4)$$

where ∇^2 and ∇_1^2 are the Laplacians with respect to material and spatial variables respectively, namely

$$\nabla^2 = \frac{\partial^2}{\partial Z^K \partial Z^K}, \quad \nabla_1^2 = \frac{\partial^2}{\partial z^i \partial z^i}, \quad (2.5)$$

and p is the pressure function occurring in Finger's stress-strain relations for the Cauchy stress tensor t^{ij} , thus

$$t^{ij} = -p \delta^{ij} + 2C_1 c^{-1ij} - 2C_2 c^{ij}, \quad (2.6)$$

and δ^{ij} is the Kronecker delta. Although, of course, (2.4) involves both the deformation and its inverse, these reciprocal equations are preferable for

complicated calculations involving fully three-dimensional deformations because they preserve the inherent symmetry of the equations of finite elasticity under interchanges of material and spatial coordinates. The strategy in utilizing reciprocal equations is to initially exploit both forms of the deformation (2.1) and then, in the final stages of the calculation, use only one of these forms. This process is demonstrated in the following section. We remark that for the neo-Hookean material ($C_2 = 0$) or for the so-called extreme Mooney material ($C_1 = 0$) we need only use one form of the deformation at the outset.

3. Solutions for compressive deformations

Together with (1.4) we utilize the inverse deformation which takes the form

$$X = F(y)x, \quad Y = G(y), \quad Z = H(y)z, \tag{3.1}$$

where F, G and H denote functions of y only such that $Ff = 1$ and $Hh = 1$. For the deformation (1.4) the incompressibility condition $|\partial z' / \partial Z^K| = 1$ becomes

$$fhg' = 1, \tag{3.2}$$

where here and subsequently primes denote differentiation with respect to Y . On introducing q defined by

$$q = p + C_2 l_2, \tag{3.3}$$

it is not difficult to show that the reciprocal equations (2.4) become

$$\left. \begin{aligned} \frac{\partial q}{\partial x} &= 2F \left\{ C_1 \frac{d^2 f}{dY^2} - C_2 \frac{d^2 F}{dy^2} \right\} x, \\ \frac{\partial q}{\partial y} &= 2 \left\{ C_1 \frac{d^2 g}{dY^2} - C_2 \left[x^2 \frac{dF}{dy} \frac{d^2 F}{dy^2} + \frac{dG}{dy} \frac{d^2 G}{dy^2} + z^2 \frac{dH}{dy} \frac{d^2 H}{dy^2} \right] \right\}, \\ \frac{\partial q}{\partial z} &= 2H \left\{ C_1 \frac{d^2 h}{dY^2} - C_2 \frac{d^2 H}{dy^2} \right\} z. \end{aligned} \right\} \tag{3.4}$$

Clearly for the second-order partial derivatives we have $q_{xz} = q_{zx} = 0$ and on equating expressions for q_{xy} and q_{zy} we obtain two equations which can be immediately integrated, thus

$$\left. \begin{aligned} F \left\{ C_1 \frac{d^2 f}{dY^2} - C_2 \frac{d^2 F}{dy^2} \right\} + C_2 \left(\frac{dF}{dy} \right)^2 &= \alpha_1, \\ H \left\{ C_1 \frac{d^2 h}{dY^2} - C_2 \frac{d^2 H}{dy^2} \right\} + C_2 \left(\frac{dH}{dy} \right)^2 &= \alpha_2, \end{aligned} \right\} \tag{3.5}$$

where α_1 and α_2 denote integration constants. On using the incompressibility condition we have

$$\frac{dF}{dy} = \frac{-hf'}{f}, \quad \frac{dH}{dy} = \frac{-fh'}{h}, \quad (3.6)$$

and (3.5) becomes

$$(C_1 + C_2h^2)f'' + C_2hh'f' = \alpha_1f, \quad (C_1 + C_2f^2)h'' + C_2ff'h' = \alpha_2h, \quad (3.7)$$

which can be readily integrated again to give

$$(C_1 + C_2h^2)f'^2 = \alpha_1f^2 + \beta_1, \quad (C_1 + C_2f^2)h'^2 = \alpha_2h^2 + \beta_2, \quad (3.8)$$

where β_1 and β_2 are further integration constants.

From the above equations it can be shown that the appropriate function $q(x, y, z)$ is given by

$$q(x, y, z) = \alpha_1x^2 + \alpha_2z^2 + C_1g'^2 - C_2\left\{x^2\left(\frac{dF}{dy}\right)^2 + \left(\frac{dG}{dy}\right)^2 + z^2\left(\frac{dH}{dy}\right)^2\right\} + p_0, \quad (3.9)$$

where p_0 is a constant. Altogether, for the pressure function $p(x, y, z)$ we find that

$$p(x, y, z) = \alpha_1f^2X^2 + \alpha_2h^2Z^2 + C_1g'^2 - C_2\left(\frac{1}{f^2} + \frac{1}{h^2}\right) - 2C_2(fh)^2\left(X^2\frac{f'^2}{f^2} + Z^2\frac{h'^2}{h^2} + 1\right) + p_0. \quad (3.10)$$

We observe that from (3.8) we have

$$dY = \left(\frac{C_1 + C_2h^2}{\alpha_1f^2 + \beta_1}\right)^{\frac{1}{2}} df = \left(\frac{C_1 + C_2f^2}{\alpha_2h^2 + \beta_2}\right)^{\frac{1}{2}} dh, \quad (3.11)$$

which although yielding the separable equation

$$\frac{df}{[(C_1 + C_2f^2)(\alpha_1f^2 + \beta_1)]^{\frac{1}{2}}} = \frac{dh}{[(C_1 + C_2h^2)(\alpha_2h^2 + \beta_2)]^{\frac{1}{2}}}, \quad (3.12)$$

in general immediately gives rise to elliptic functions (except in the special case when $\alpha_1/\beta_1 = \alpha_2/\beta_2 = C_2/C_1$). We further note that if $f \equiv h$ (and $\alpha_1 = \alpha_2$, $\beta_1 = \beta_2$) then (1.4) is essentially the axially symmetric deformation studied by Klingbeil and Shield (2) in the context of squashing circular pads of rubber and these authors also noted that the particular deformation studied resulted in elliptic functions for the Mooney material. Finally in this section, for the neo-Hookean material ($C_2 = 0$) we have immediately from (3.11) that

$$dY = \frac{C_1^{\frac{1}{2}} df}{(\alpha_1f^2 + \beta_1)^{\frac{1}{2}}} = \frac{C_1^{\frac{1}{2}} dh}{(\alpha_2h^2 + \beta_2)^{\frac{1}{2}}}, \quad (3.13)$$

which readily yield simple trigonometric functions as solutions for f and h , while for the extreme Mooney material ($C_1 = 0$), (3.6) and (3.8) give

$$dy = \frac{C_2^{\frac{1}{2}} dF}{(\alpha_1 + \beta_1 F^2)^{\frac{1}{2}}} = \frac{C_2^{\frac{1}{2}} dH}{(\alpha_2 + \beta_2 H^2)^{\frac{1}{2}}}, \tag{3.14}$$

which again results in simple trigonometric functions, the explicit nature of which depends on the signs of the various integration constants. In the following section we detail such solutions appropriate to the compressing of rectangular pads.

4. Approximate analysis for compression of finite rectangular blocks

We consider a rectangular rubber block with undeformed dimensions of length $2L$, breadth $2B$ and thickness $2T$ as indicated in Fig. 2. We suppose that in the undeformed state the rectangular Cartesian coordinate system (X, Y, Z) has its origin located at the central point of the block and that the faces $Y = \pm T$ have bonded rigid metal plates over which there is an applied normal force F resulting in a final thickness $2t$. Assuming a deformation of the form (1.4), we require that f and h are even while g is an odd function. In addition we require that

$$f(\pm T) = 1, \quad g(\pm T) = \pm t, \quad h(\pm T) = 1. \tag{4.1}$$

We assume that the pointwise zero-stress conditions on the free surfaces $Z = \pm L$ and $X = \pm B$ can be approximated by the vanishing of force resultants on these surfaces, and because of the symmetries of f, g and h these become

$$\int_{-L}^L \int_{-T}^T T_R^{11} dZ dY = 0, \quad \int_{-B}^B \int_{-T}^T T_R^{33} dX dY = 0, \tag{4.2}$$

on surfaces $X = \pm B$ and $Z = \pm L$ respectively. In addition the applied normal force on the metal end-plates is given by

$$F = - \int_{-B}^B \int_{-L}^L T_R^{22} dX dZ, \tag{4.3}$$

where T_R^{KJ} denotes the first Piola-Kirchhoff stress tensor with components

$$\left. \begin{aligned} T_R^{11} &= -pg'h + 2C_1f - 2C_2g'h^3(g'^2 + f'^2X^2), \\ T_R^{22} &= -pfh + 2C_1g' - 2C_2fh[(f^2 + f'^2X^2)h^2 + (fh')^2Z^2], \\ T_R^{33} &= -pg'f + 2C_1h - 2C_2g'f^3(g'^2 + h'^2Z^2), \\ T_R^{12} &= \{p + 2C_2[(f^2 + g'^2 + f'^2X^2)h^2 + (fh')^2Z^2]\}f'hX, \\ T_R^{32} &= \{p + 2C_2[(h^2 + g'^2 + h'^2Z^2)f^2 + (f'h)^2X^2]\}fh'Z, \\ T_R^{21} &= 2(C_1 + C_2h^2)f'X, \quad T_R^{23} = 2(C_1 + C_2f^2)h'Z, \\ T_R^{13} &= -2C_2ff'h'XZ, \quad T_R^{31} = -2C_2hf'h'XZ. \end{aligned} \right\} \tag{4.4}$$

From the above equations is it not difficult to deduce the expression for the applied force F , namely

$$F = -4BL \left\{ C_1 + 2C_2 - \frac{\alpha_1 B^2}{3} - \frac{\alpha_2 L^2}{3} - p_0 \right\}. \quad (4.5)$$

If we introduce the mid-plane stretches λ_1 and λ_2 such that

$$\lambda_1 = f(0), \quad \lambda_2 = h(0), \quad (4.6)$$

then using the fact that $f'(0)$ and $h'(0)$ are zero we see that $\beta_1 = -\alpha_1 \lambda_1^2$, $\beta_2 = -\alpha_2 \lambda_2^2$ and equation (3.8) becomes

$$(C_1 + C_2 h^2) f'^2 = \alpha_1 (f^2 - \lambda_1^2), \quad (C_1 + C_2 f^2) h'^2 = \alpha_2 (h^2 - \lambda_2^2). \quad (4.7)$$

In principle for a given applied force F the five conditions (4.1)₁, (4.1)₃, (4.2)₁, (4.2)₂ and (4.3) constitute five equations for the determination of the five unknown constants α_1 , α_2 , λ_1 , λ_2 and p_0 from which a theoretical value for the new thickness $2t$ can be predicted. In the remainder of this section we consider the neo-Hookean material for which solutions of (4.7) can be given explicitly, and numerical results for this material are given in section 6.

If $C_2 = 0$ then it can be shown that the appropriate solutions of (4.7) are

$$f(Y) = \lambda_1 \cos k_1 Y, \quad h(Y) = \lambda_2 \cos k_2 Y, \quad (4.8)$$

where the constants k_1 and k_2 are related to α_1 and α_2 as follows:

$$k_1^2 = -\alpha_1 / C_1, \quad k_2^2 = -\alpha_2 / C_1. \quad (4.9)$$

Further, from (3.2) we may deduce that

$$g(Y) = \frac{1}{\lambda_1 \lambda_2} \int_0^Y \sec k_1 \xi \sec k_2 \xi \, d\xi, \quad (4.10)$$

while (4.1) gives

$$\left. \begin{aligned} \lambda_1 &= \sec k_1 T, & \lambda_2 &= \sec k_2 T, \\ t &= \frac{1}{\lambda_1 \lambda_2} \int_0^T \sec k_1 \xi \sec k_2 \xi \, d\xi. \end{aligned} \right\} \quad (4.11)$$

Further for the neo-Hookean material the conditions (4.2) and (4.5) become

$$\left. \begin{aligned} & \frac{p_0}{C_1} \int_0^T \left(\frac{\sec k_1 \xi}{\sec k_1 T} \right) d\xi + \int_0^T \left(\frac{\sec k_1 \xi}{\sec k_1 T} \right)^3 \left(\frac{\sec k_2 \xi}{\sec k_2 T} \right)^2 d\xi \\ & = (2 + k_1^2 B^2) \frac{\tan k_1 T}{k_1} + \frac{k_2^2 L^2}{3} \int_0^T \left(\frac{\sec k_1 \xi}{\sec k_1 T} \right) \left(\frac{\sec k_2 \xi}{\sec k_2 T} \right)^2 d\xi, \end{aligned} \right\}$$

$$\left. \begin{aligned} & \frac{p_0}{C_1} \int_0^T \left(\frac{\sec k_2 \xi}{\sec k_2 T} \right) d\xi + \int_0^T \left(\frac{\sec k_2 \xi}{\sec k_2 T} \right)^3 \left(\frac{\sec k_1 \xi}{\sec k_1 T} \right)^2 d\xi \\ & = (2 + k_2^2 L^2) \frac{\tan k_2 T}{k_2} + \frac{k_1^2 B^2}{3} \int_0^T \left(\frac{\sec k_2 \xi}{\sec k_2 T} \right) \left(\frac{\sec k_1 \xi}{\sec k_1 T} \right)^2 d\xi, \\ & \frac{F}{C_1} = 4BL \left\{ 1 + \frac{k_1^2 B^2}{3} + \frac{k_2^2 L^2}{3} - \frac{p_0}{C_1} \right\}. \end{aligned} \right\} (4.12)$$

In principle these three equations constitute three equations for the three unknowns k_1 , k_2 and p_0 which in general need to be solved numerically. However in the special case when $L = B$ we have the following simplifications resulting from (4.11) and (4.12):

$$\left. \begin{aligned} & k_1 = k_2 = k, \quad \lambda_1 = \lambda_2 = \sec kT, \quad t = \frac{\sin 2kT}{2k}, \\ & \left\{ \frac{p_0}{C_1} + \frac{3}{8} \cos^4 kT \right\} \log [\sec kT + \tan kT] \\ & = \left\{ 2 \left(1 + \frac{2k^2 B^2}{3} \right) - \frac{1}{4} \cos^2 kT - \frac{3}{8} \cos^4 kT \right\} \tan kT \sec kT, \\ & \frac{F}{C_1} = 4BL \left\{ 1 + \frac{2k^2 B^2}{3} - \frac{p_0}{C_1} \right\}. \end{aligned} \right\} (4.13)$$

These results are displayed numerically in section 6. Finally in this section we note that similar formulae can also be deduced for the extreme Mooney material ($C_1 = 0$). However since this strain-energy function has no real physical basis we do not give these results here.

5. Linear estimate and the shape-factor method

For small compression we define the applied strain $e = (T - t)/T$ and we suppose that the deformation and stresses can be expanded in powers of e so that consistently neglecting e^2 and higher powers gives the usual linear theory of elasticity. Thus for the deformation we have

$$\left. \begin{aligned} & f(Y) = 1 + eu(Y) + \dots = 1 + e\gamma_1(T^2 - Y^2) + \dots, \\ & g(Y) = Y + ev(Y) + \dots = Y + e(\gamma_1 + \gamma_2) \left(\frac{Y^3}{3} - T^2 Y \right) + \dots, \\ & h(Y) = 1 + ew(Y) + \dots = 1 + e\gamma_2(T^2 - Y^2) + \dots, \end{aligned} \right\} (5.1)$$

while for the pressure function and diagonal stress components we have

$$\begin{aligned} p(X, Y, Z) &= 2(C_1 - C_2) + eP(X, Y, Z) + \dots \\ &= 2(C_1 - C_2) + e\mu[\gamma_1(Y^2 - X^2) + \gamma_2(Y^2 - Z^2) + \gamma_3] + \dots, \end{aligned} \quad (5.2)$$

and

$$\left. \begin{aligned} T_R^{11} &= e[-P + 2\mu\mu] + \dots, & T_R^{22} &= e[-P + 2\mu\nu'] + \dots, \\ T_R^{33} &= e[-P + 2\mu w] + \dots, \end{aligned} \right\} \quad (5.3)$$

where γ_1 , γ_2 and γ_3 denote arbitrary constants and $\mu = 2(C_1 + C_2)$ is the linear shear modulus. Now from the above, (4.2) and (4.3) we may deduce the two equations,

$$3\gamma_1(T^2 + B^2) - \gamma_2(T^2 - L^2) = 3\gamma_3, \quad 3\gamma_2(T^2 + L^2) - \gamma_1(T^2 - B^2) = 3\gamma_3, \quad (5.4)$$

which have solutions

$$\left. \begin{aligned} \gamma_1 &= \frac{3\gamma_3(L^2 + 2T^2)}{[5T^2(L^2 + B^2) + 4(T^4 + L^2B^2)]}, \\ \gamma_2 &= \frac{3\gamma_3(B^2 + 2T^2)}{[5T^2(L^2 + B^2) + 4(T^4 + L^2B^2)]}. \end{aligned} \right\} \quad (5.5)$$

But from the definition of the applied strain e we may deduce that $v(T) = -T$ and thus we have

$$2T^2(\gamma_1 + \gamma_2) = 3, \quad (5.6)$$

which together with (5.5) is the determining equation for γ_3 , thus

$$\gamma_3 = \frac{[5T^2(L^2 + B^2) + 4(T^4 + L^2B^2)]}{2T^2(L^2 + B^2 + 4T^2)}. \quad (5.7)$$

Now, from (4.3) and (5.3)₂, we have

$$F = \frac{4\mu BLe}{3} \{(3T^2 - B^2)\gamma_1 + (3T^2 - L^2)\gamma_2 + 3\gamma_3\}, \quad (5.8)$$

which, on using the above equations, simplifies to give

$$\frac{F}{4BL} = \frac{Ee}{3} \left\{ 1 + \frac{(B^2 + 2T^2)(L^2 + 2T^2)}{(B^2 + L^2 + 4T^2)T^2} \right\}, \quad (5.9)$$

where E is the linear Young's modulus, that is

$$E = 6(C_1 + C_2) = 3\mu. \quad (5.10)$$

We observe that in the limit as L tends to infinity (5.9) agrees with the expression given by Klingbeil and Shield (2) resulting from their plane-strain analysis for long rubber blocks.

Lindley (5) and Gent and Meinecke (6) propose shape-factor methods for the compression of rectangular rubber blocks which utilize equations (1.1) and (1.2). For a compression of magnitude δ we have

$$\delta = 2T - 2t = 2Te, \quad (5.11)$$

where $e = (T - t)/T$ is the applied strain. Now the shape factor as defined

by (1.1) at a compression of magnitude δ is 'approximately'

$$S = \frac{4BL}{2(4Lt + 4Bt)} = \frac{S_0}{(1-e)}, \quad (5.12)$$

where S_0 is the original shape factor of the rectangular rubber block. Now the shape-factor methods for rectangular blocks with $B \leq L$ are based on assuming that the apparent Young's modulus E_a in (1.2) takes the form

$$E_a = E_h + ECS^2, \quad (5.13)$$

where E is the linear Young's modulus, C is a constant given by

$$C = \frac{4}{3} + \frac{B}{L} \left(2 - \frac{11B}{10L} \right), \quad (5.14)$$

and E_h is known as the 'homogeneous' compression modulus. Lindley (5) proposes the expression

$$E_h = E \left\{ 1 + \frac{1}{3} \left(\frac{L^2 - B^2}{L^2 + B^2} \right)^2 \right\}, \quad (5.15)$$

while Gent and Meinecke (6) suggest an alternative expression:

$$E_h = E \left\{ 1 + \frac{1}{3} \frac{(L-B)^2}{(L^2 + B^2 + 8T^2)} \right\}. \quad (5.16)$$

We observe that both expressions yield the linear Young's modulus if $B = L$ while both predict the plane strain limit $4E/3$ for L tending to infinity. Now from (1.2) we have

$$\frac{dF}{d\delta} = \frac{4BLE_a}{(2T - \delta)}, \quad (5.17)$$

and thus from (5.11) to (5.13) we may deduce that

$$\frac{dF}{de} = 4BL \left\{ \frac{E_h}{(1-e)} + \frac{ECS_0^2}{(1-e)^3} \right\}. \quad (5.18)$$

Hence, on integration with respect to e and using the fact that the applied strain e is zero when F is zero, we obtain

$$F = 4BL \left\{ \frac{ECS_0^2}{2(1-e)^2} - E_h \log(1-e) - \frac{ECS_0^2}{2} \right\}. \quad (5.19)$$

For small applied strains this gives

$$F = 4BLE \{ E_h + ECS_0^2 \}. \quad (5.20)$$

Equation (5.19) with Lindley's expression (5.15) for E_h is used for the numerical work in the following section.

Finally in this section we simply note that if we also allow a variation with compression of the homogeneous compression modulus (5.16), thus

$$E_h^* = E \left\{ 1 + \frac{(L-B)^2}{3(L^2 + B^2 + 8t^2)} \right\}, \quad (5.21)$$

then (5.18) can still be integrated, with E_h^* in place of E_h , with the result that

$$F^* = 4BL \left\{ \frac{ECS_0^2}{2(1-e)^2} + \frac{E(L-B)^2}{6(L^2+B^2)} \log \left[\frac{1+(L^2+B^2)/8T^2(1-e)^2}{1+(L^2+B^2)/8T^2} \right] - E \log(1-e) - \frac{ECS_0^2}{2} \right\}, \quad (5.22)$$

which actually gives almost identical results to (5.19) with Lindley's expression (5.15) for the homogeneous compression modulus.

6. Experimental and numerical results

We first compare numerical values of the applied force for the finite model for the neo-Hookean material with the plane-strain approximation given by Klingbeil and Shield (2). Table 1 gives numerical values of F for six blocks each of thickness 10 cm, breadth 20 cm and lengths ranging from 30 cm to 960 cm and a shear modulus $\mu = 0.064 \text{ kN/cm}^2$. Interestingly enough the three-dimensional deformation produces results which tend to those of Klingbeil and Shield (2) as the length of the block tends to infinity. Although this is a highly desirable feature it is not altogether obvious why this should happen because the finite model has an additional constraint (namely (4.2)₂) over the end-faces of the block. No such constraint exists for the Klingbeil and Shield (2) model and the authors are not entirely clear why (4.2)₂ becomes redundant as $2L$ tends to infinity. For the neo-Hookean material, the length L tending to infinity corresponds to the constant k_2 tending to zero and formally the two conditions (4.12) are compatible because the product k_2L remains finite. In the limit as L tends to infinity and k_2 tends to zero, (4.12) gives

$$\left. \begin{aligned} \frac{p_0}{C_1} - \frac{(k_2L)^2}{3} &= \left\{ 2 + (k_1B)^2 - \frac{1}{2\lambda_1^2} \right\} \frac{\tan k_1T}{k_1t} - \frac{1}{2\lambda_1^2}, \\ \frac{p_0}{C_1} - (k_2L)^2 &= 2 + \left\{ \frac{(k_1B)^2}{3} - 1 \right\} \frac{\tan k_1T}{\lambda_1^2 k_1T}, \end{aligned} \right\} \quad (6.1)$$

and these two equations together fix the product k_2L . However, (6.1)₁ is the condition used by Klingbeil and Shield (2) and since the quantity on the left-hand side of this equation also appears in the expression (4.12)₃ for the applied force F , we have at least some explanation why the numerical results of Table 1 coincide for long blocks.

In order to make an objective assessment of the various force-deflection relations for the compression of rectangular blocks we need to prescribe the linear shear modulus μ or Young's modulus E ($E = 3\mu$). In this regard, we can either adopt the strategy that for each force-deflection relation E is a variable parameter of the model determined from linear experimental data,

TABLE 1. Comparison of applied forces for the finite-block model for the neo-Hookean material and (2) for six blocks each of thickness 10 cm, breadth 20 cm and lengths increasing from 30 cm to 960 cm for a shear modulus of 0.064 kN/cm²

Strain	Force (kN)					
	2L = 30 cm	2L = 60 cm	2L = 120 cm	2L = 240 cm	2L = 480 cm	2L = 960 cm
	(4.12)	(2)	(4.12)	(2)	(4.12)	(2)
0.04	8	12	45	93	187	375
0.08	17	26	98	202	408	818
0.12	27	42	161	333	671	1347
0.16	39	62	235	489	987	1980
0.20	52	86	324	676	1368	2746
0.24	68	115	432	904	1830	3672
0.28	86	150	561	1181	2396	4808
0.32	108	194	720	1522	3093	6210

TABLE 2. Values of shear modulus for varying hardness from Lindley (7), Payne and Scott (8), Göbel (9) and British Standard data (BS5400)

Hardness (IRHD)	Shear modulus (kN/cm ²)			
	Lindley (7)	Payne and Scott (8)	Göbel (9)	British Standard
30	0.030	0.033	—	—
40	0.045	0.053	0.047	—
50	0.064	0.074	0.071	0.060
60	0.106	0.110	0.096	0.090
70	0.173	0.174	0.134	0.120
80	—	0.310	0.191	—

in which case we obtain a different value for each theory, or we can independently measure the hardness of the rubber block and obtain the shear or Young's modulus from tables. For our own experimental results we adopt both points of view and give two sets of graphs. In our analysis of the experimental results of Gent and Lindley (1) we adopt the former approach. The shear modulus of rubber is related to its hardness and there are various hardness systems including International Rubber Hardness Degrees (IRHD), Shore and British Standard Hardness. In our experiments the hardness of the rubber blocks was measured using a Shore durometer (model A) which actually gives values which are almost the same as those from the IRHD system. Various authors provide information which relates hardness to shear modulus (see for example Lindley (7), Payne and Scott (8), Göbel (9) and Table 2).

The data provided by Lindley (7) results from experiments on natural rubber springs with hardness above 48 IRHD and measured at low shear strain. Lindley (7) maintains that hardness measurements are subject to some uncertainty and states that there should be ± 2 degrees tolerance in hardness in Table 2. Payne and Scott (8) claim that their data form an ideal relationship and that a difference of 1 degree in hardness corresponds to approximately 4.5 per cent difference in modulus. Göbel (9) does not give any details about his data and the British Standard data (BS5400) is based on shear strains ranging from 5 to 25 per cent.

Before proceeding to our own experimental work we first compare our results with existing experimental results of Gent and Lindley (1). Table 3 gives experimental values of $F/4BL$ for four square blocks of varying shape factor S_0 . The experimental values are obtained from (magnified) graphical results and accordingly while they are not completely precise they are nevertheless reasonably accurate. The values of the Young's modulus used in the table are obtained from the initial linear portion of the curves given in (1) and the formulae

$$\frac{F}{4BL} = Ee \left(1 + \frac{16}{3} S_0^2 \right), \quad \frac{F}{4BL} = Ee \left(1 + \frac{67}{30} S_0^2 \right), \quad \frac{F}{4BL} = \frac{2}{3} Ee (1 + 4S_0^2), \quad (6.2)$$

TABLE 3. *Experimental results of Gent and Lindley (1) compared with Klingbeil and Shield (2) and the present model for the neo-Hookean material*

Shape factor S_0	Percentage strain	Force per unit area ($F/4BL$)(kgf/cm ²)			
		(2)	Experimental (1)	Shape factor (5.20)	Finite neo-Hookean (4.12)
0.18	10	2.6	2.3	2.4	2.4
	20	6.2	5.3	5.2	5.2
	30	11.3	9.4	8.7	8.7
0.39	10	3.4	2.8	3.0	3.1
	20	8.5	6.4	6.7	7.2
	30	16.6	12.0	11.2	12.6
0.51	10	4.2	3.4	3.7	3.9
	20	10.9	7.6	8.3	9.2
	30	21.8	14.2	14.2	16.6
0.85	10	6.5	5.0	5.6	6.0
	20	17.3	11.8	13.0	14.7
	30	35.6	20.8	22.9	27.8

being the appropriate linear approximations for the Klingbeil and Shield (2) estimate, the shape factor estimate (see (5.20), (5.14) and (5.15)) and the present work (see (5.9)) respectively where for the square block $S_0 = B/4T$. The actual values of E used in Table 3 are given in Table 4 and result from the given experimental results in Table 3 at 10 per cent strain. For the finite model, results for only the neo-Hookean material are given. It is apparent from the table that the full three-dimensional approximation presented here is considerably superior to the Klingbeil and Shield (2) model but bear in mind the latter model is at its worst for the square block. We also observe from the table that the shape-factor estimate appears to provide a consistently good approximation.

In order to obtain a more objective assessment of the situation we

TABLE 4

Shape factor S_0	Young's modulus E (kgf/cm ²)		
	(6.2) ₁	Shape factor (6.2) ₂	Finite (6.2) ₃
0.18	19.61	21.45	30.54
0.39	15.46	20.90	26.11
0.51	14.24	21.51	25.00
0.85	10.30	19.13	19.28

TABLE 5

Figure	Young's modulus E (kN/cm ²)			Figure	Young's modulus E (kN/cm ²)	
	(2)	Shape factor	Finite		(2) and finite	Shape factor
3(a)	0.1767	0.2355	0.2533	3(b)	0.1863	0.1710
4(a)	0.5897	0.7263	0.9573	4(b)	0.5793	0.3870
5(a)	0.1613	0.2463	0.2603	5(b)	0.1920	0.1800
6(a)	0.2005	0.2517	0.2875	6(b)	0.1983	0.1845

conducted experiments on rubber blocks using a hydraulic compression testing machine. For forces in the range 0 to 2000 kN the machine measures hydraulic pressure. However, for forces in the range 0 to 200 kN a load cell can be inserted to obtain more accurate results. The hydraulic compressor has an accuracy of ± 10 to 15 per cent in the range 0 to 2000 kN while the 200 kN load cell has an accuracy of ± 5 per cent. Sandpaper was used to simulate a bonded rubber block and the area of contact between the rubber and the compressing metal plates remained substantially constant. The force measurements were displayed digitally and the deflection was read from four dial gauges situated at the corners of the compressing metal plates. The average of these four readings was taken as the deflection which took place. The Young's modulus used in the theoretical curves of Figs 3(a), 4(a), 5(a) and 6(a) are obtained from the initial linear portion of the experimental curves. Table 5 gives the values of the Young's modulus obtained in this manner and also the value of the Young's modulus obtained by measuring the hardness of the rubber and using Table 2. For the Klingbeil and Shield approximation and the present estimate the Young's modulus in Table 5 arising from the hardness test is that obtained from Lindley (7) while the value given in Table 5 for the shape-factor approximation is that obtained using British Standard data which is generally used in conjunction with this estimate. From Figs 3(a), 4(a), 5(a) and 6(a) it is apparent that although the finite model is an improvement on the Klingbeil and Shield estimate, the shape-factor approximation appears to be superior to both. However, if we adopt the alternative strategy and assign each theory the value of E , obtained from the hardness test, then Figs 3(b), 4(b), 5(b) and 6(b) appear to indicate that the finite model is superior to both the Klingbeil and Shield estimate and the shape-factor approximation.

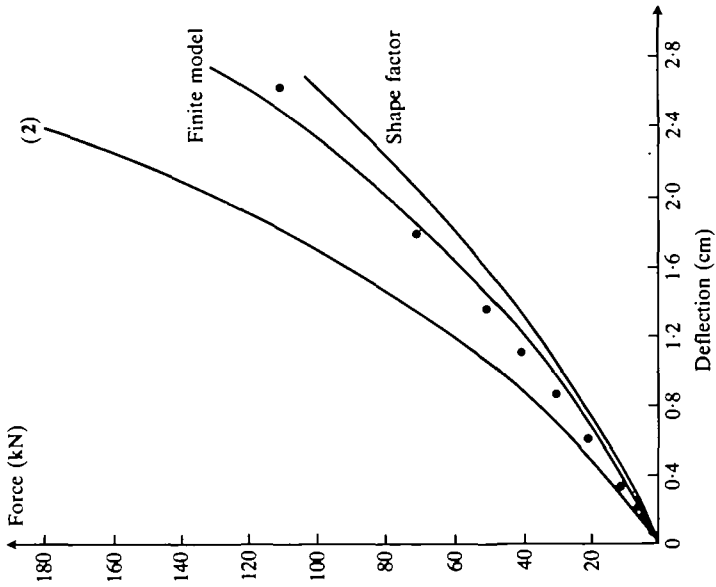


FIG. 3(b)

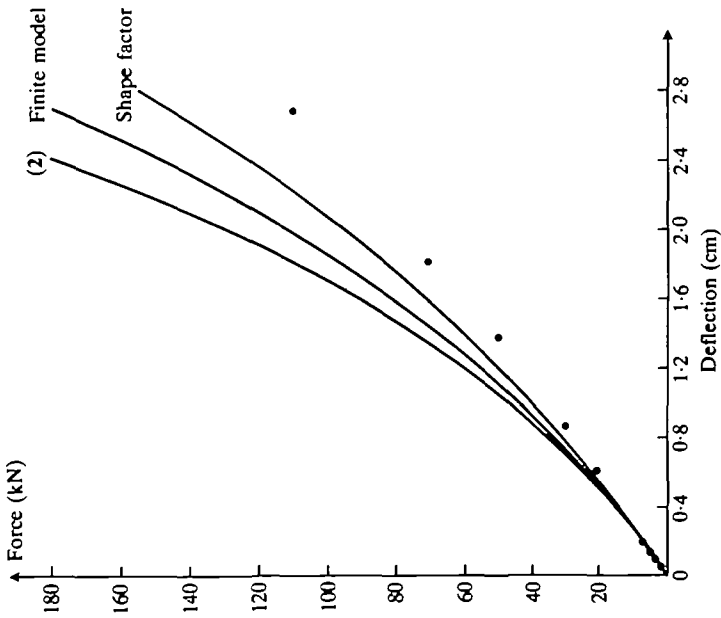


FIG. 3(a)

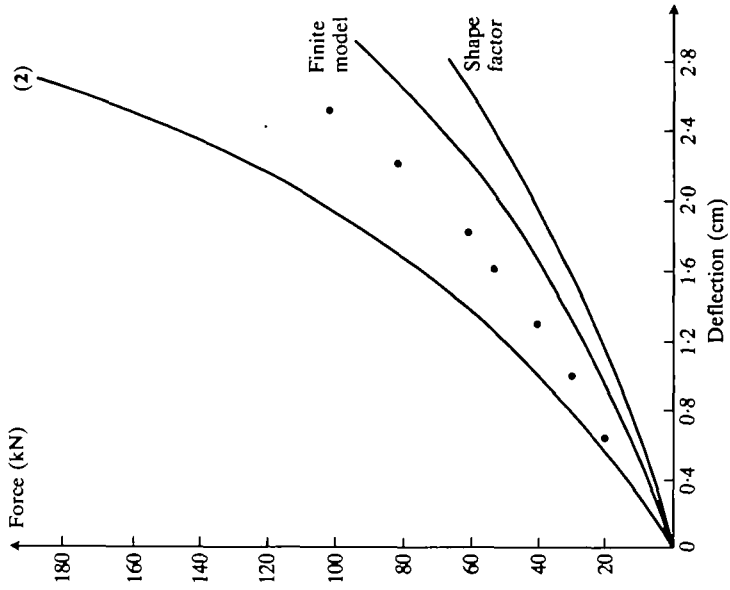


FIG. 4(b)

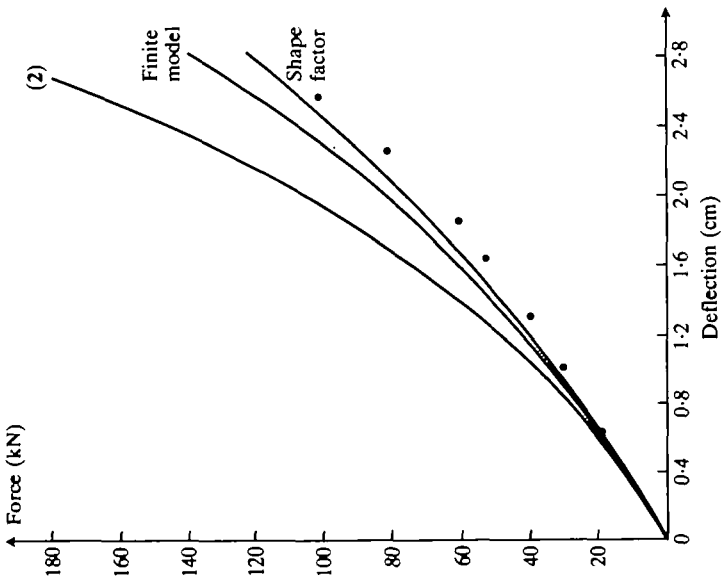


FIG. 4(a)

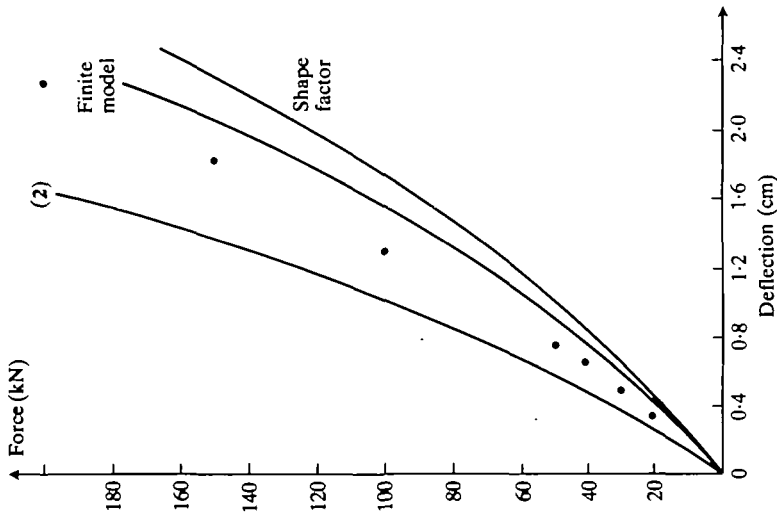


FIG. 5(b)

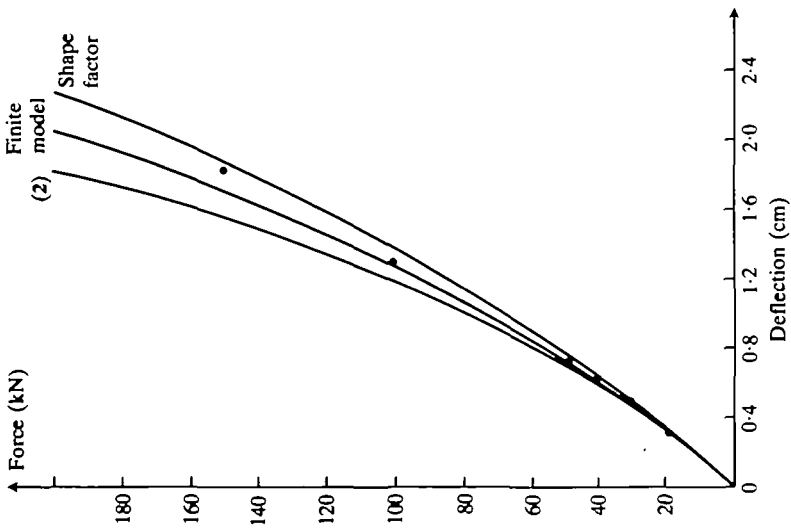


FIG. 5(a)

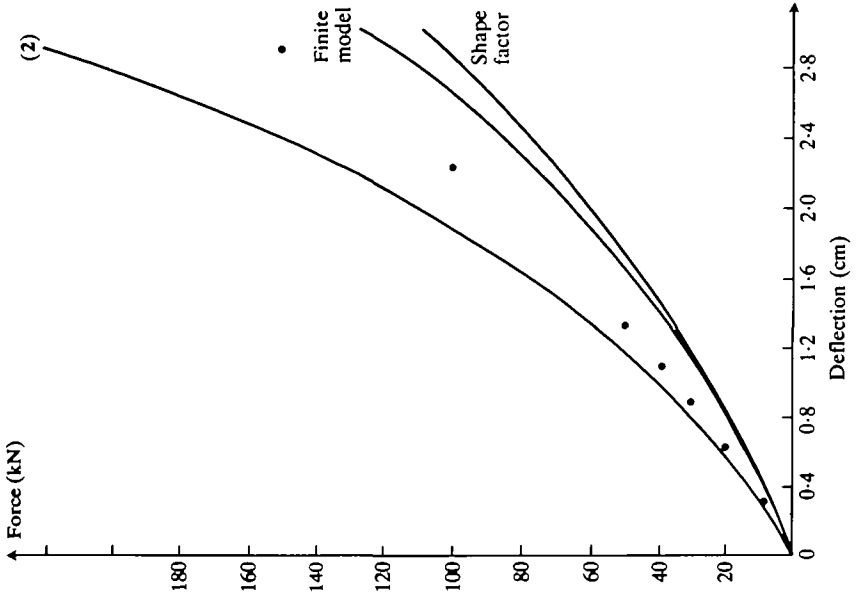


FIG. 6(b)

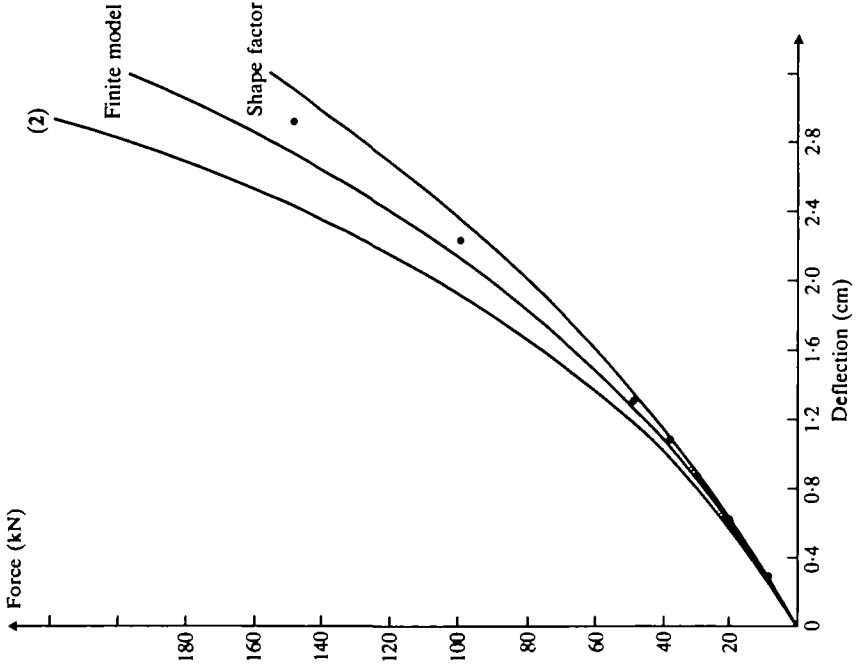


FIG. 6(a)

7. Conclusion

In modelling the compression of rectangular rubber blocks, we have utilized a three-dimensional deformation for the isotropic incompressible perfectly elastic Mooney material, to generate an approximate solution of the problem, for which the pointwise vanishing of the stress on free surfaces is approximated by the vanishing of force resultants over the surface. This new approximation appears to be a substantial improvement on a similar approximation due to Klingbeil and Shield (2) which is strictly only valid for extremely long rubber blocks. Moreover we have compared the new load-deflection relation with new experimental data and with results arising from the shape-factor approximation which is commonly used in engineering. Our work tends to indicate that if the shape-factor approximation is used in conjunction with a value of the Young's modulus obtained from the linear experimental data then this generates a consistently good estimate. However, our work also indicates that the finite model presented here also provides a reasonably accurate approximation irrespective of whether the Young's modulus is determined from the linear experimental data or from a hardness test. The related problem of combined compression and torsion of circular cylindrical bonded rubber mounts is examined in a companion paper (10).

Acknowledgements

The second author gratefully acknowledges the financial support of an Australian National Research Fellowship. This work has been undertaken as a part of a collaborative research programme with the Sydney manufacturer of rubber engineering components P. J. O'Connor. The authors are extremely grateful for the use of their testing facilities and particularly to the Manager, Mr Peter Snowball, who has enthusiastically assisted the programme.

REFERENCES

1. A. N. GENT and P. B. LINDLEY, *Proc. Instn mech. Engng* **173** (1959) 111-117.
2. W. W. KLINGBEIL and R. T. SHIELD, *Z. angew. Math. Phys.* **17** (1966) 281-305.
3. J. M. HILL, *ibid.* **24** (1973) 609-618.
4. —, Ph.D. thesis, Queensland University, Australia 1972.
5. P. B. LINDLEY, *Plastics and Rubber Processing and Applications* **1** (1981) 331-337.
6. A. N. GENT and E. A. MEINECKE, *Poly. Eng. Sci.* **10** (1970) 48-53.
7. P. B. LINDLEY, *Engineering Design with Natural Rubber*. Natural Rubber Technical Bulletin (1966).
8. A. R. PAYNE and J. R. SCOTT, *Engineering Design with Rubber* (Maclaren, London 1960).
9. E. F. GÖBEL, *Rubber Springs Design* (Newnes-Butterworths, London 1974).
10. J. M. HILL and A. I. LEE, *J. Mech. Phys. Solids* to appear.